Cancer Chemother Pharmacol (2012) 69:1051–1061
DOI 10.1007/s00280-011-1803-9

ORIGINAL ARTICLE

Afatinib pharmacokinetics and metabolism after oral administration to healthy male volunteers

Peter Stopfer · Kristell Marzin · Hans Narjes · Dietmar Gansser · Mehdi Shahidi · Martina Uttereuther-Fischer · Thomas Ebner

Received: 26 October 2011 / Accepted: 12 December 2011 / Published online: 27 December 2011

Abstract
Purpose To investigate the pharmacokinetics, metabolism and tolerability of afatinib (BIBW 2992), an oral irreversible ErbB family blocker, in healthy male volunteers.
Methods In this open-label, single-center study, 8 healthy male volunteers received a single oral dose of 15 mg [^{14}C]-radiolabeled afatinib (equivalent to 22.2 mg of the dimaleinate salt) as a solution. Blood, urine and fecal samples were collected for at least 96 hours (h) after dosing. Plasma and urine concentrations of afatinib were analyzed using high-performance liquid chromatography–tandem mass spectrometry. [^{14}C]-radioactivity levels in plasma, whole blood, urine and feces were measured by liquid scintillation counting methods. Metabolite patterns were assessed by high-performance liquid chromatography.
Results [^{14}C]-radioactivity was mainly excreted via feces (85.4%). Overall recovery of [^{14}C]-radioactivity was 89.5%, indicative of a complete mass balance. Afatinib was slowly absorbed, with maximum plasma concentrations achieved at a median of 6 h after dosing, declining thereafter in a biexponential manner. The geometric mean terminal half-life of afatinib was 33.9 h in plasma and longer for [^{14}C]-radioactivity in plasma and whole blood. Apparent total body clearance for afatinib was high (geometric mean 1,530 mL/min). The high volume of distribution (4,500 L) in plasma may indicate a high tissue distribution. Afatinib was metabolized to only a minor extent, with the main metabolite afatinib covalently bound to plasma proteins. Oxidative metabolism mediated via cytochrome P-450 was of negligible importance for the elimination of afatinib. Afatinib was well tolerated.
Conclusions Afatinib displayed a complete mass balance with the main route of excretion via feces. Afatinib undergoes minimal metabolism.

Keywords Afatinib · BIBW 2992 · Metabolism · Excretion · Pharmacokinetics · Human

P. Stopfer (✉) · K. Marzin · H. Narjes · D. Gansser · M. Uttereuther-Fischer · T. Ebner
Boehringer Ingelheim Pharma GmbH & Co. KG, Birkendorfer Strasse, 88400 Biberach an der Riss, Germany
e-mail: Peter.Stopfer@boehringer-ingelheim.com

M. Shahidi
Boehringer Ingelheim, Bracknell, UK

Introduction

Afatinib (BIBW 2992), is an oral, highly selective, potent and irreversible ErbB family blocker, inhibiting ErbB1 (epidermal growth factor receptor [EGFR]/human epidermal growth factor receptor [HER]1) (IC_{50} 0.5 nM), ErbB2 (HER2) (IC_{50} 14 nM) and ErbB4 (HER4) (IC_{50} 1 nM) [1, 2] (and Boehringer Ingelheim, data on file). As these receptors are involved in cell proliferation, differentiation and apoptosis, their inhibition may play a critical role in the prevention of tumor growth and spread. Afatinib is in clinical development for the management of several types of solid tumors, including non-small cell lung cancer (NSCLC), breast and head and neck cancer.

Previous phase I studies in patients with advanced solid tumors showed that afatinib had a manageable side effect profile when administered as monotherapy [3–6] or in combination with other cancer therapies including paclitaxel [7], docetaxel [8], vinorelbine [2], cisplatin/paclitaxel and cisplatin/5-fluorouracil [9]. Promising results from phase II and phase IIb/III clinical trials in patients with relapsed advanced NSCLC cancer [10, 11] and metastatic breast cancer [12] suggest potential benefit with afatinib

monotherapy. In patients with advanced NSCLC who harbor EGFR mutations, use of afatinib led to an overall response rate (ORR) of 57% by independent review and 61% by investigator assessment, with a high ORR rate seen across the main subgroups [11]. In patients with advanced NSCLC whose disease has progressed after receiving chemotherapy and a first-generation EGFR tyrosine kinase inhibitor (gefitinib or erlotinib), afatinib treatment demonstrated a statistically significant progression-free survival benefit over placebo (3.3 months vs. 1.1 months) [10].

Pharmacokinetic studies in patients with advanced solid tumors showed that dose-dependent concentrations of afatinib are achieved after oral administration [5, 6]. Maximum plasma levels of afatinib are generally reached within 3–5 h after oral dosing. As the terminal half-life after single-dose administration ranged from 22 to 40 h, afatinib is therefore suitable for once-daily dosing [5, 6]. A relatively high apparent total body clearance and volume of distribution were observed. While these values should be treated with caution, as the absolute bioavailability of afatinib in humans is unknown, these data suggest that afatinib has a suitable elimination profile and a high tissue distribution. All pharmacokinetic parameters displayed moderate-to-high variability, although within the expected range compared with other EGFR tyrosine kinase inhibitors [13–16]. Steady state is attained within 7 days after the start of multiple once-daily dosing [6].

Non-clinical metabolism studies in several animal species have revealed that afatinib undergoes minor metabolism in quantitative terms. Overall, metabolism as excretion pathway was of subordinate importance compared with excretion of unchanged parent compound in the mouse, rat, minipig and rabbit (Boehringer Ingelheim, data on file) with only minor differences in the metabolite pattern between species. The in vitro metabolic profile of afatinib suggests that it does not interact in a relevant way with cytochrome P-450 (CYP450) enzymes and does not inhibit (reversibly or irreversibly) or induce CYP450 enzymes (Boehringer Ingelheim, data on file).

The aim of this study was to characterize the pharmacokinetics (including the excretion pathways and mass balance) and metabolism of afatinib after single oral administration to healthy male volunteers.

Materials and methods

Study design

This was an open-label, single-dose study performed at Pharma Bio-Research Group BV (Zuidlaren, The Netherlands). The study was approved by an independent ethics committee (Medische Ethische Toetsings Commissie van de Stichting Beoordeling Bio-Medisch Onderzoek, Assen, The Netherlands) and conducted according to the principles of Good Clinical Practice and the Declaration of Helsinki (October 1996 version). Written informed consent was obtained from all participants before study entry.

Study population

The pharmacokinetics and metabolism of afatinib were studied in 8 healthy male volunteers (7 Caucasians and 1 Asian), with mean age 50.4 years (range 35–60 years), mean weight 80.1 kg (range 64–101 kg) and mean body mass index 25.1 kg/m^2 (range 22.4–29.3 kg/m^2). All 8 subjects completed the study according to protocol.

Radiolabeling of afatinib dimaleinate salt

[^{14}C]-afatinib dimaleinate salt was synthesized by introducing the radiolabel into position 2 of the quinazoline ring.

Treatment regimens

After an overnight fast (at least 10 h), subjects received a single oral 15 mg dose (calculated as the free base) of afatinib (equivalent to 22.2 mg of afatinib dimaleinate salt) solution containing 2.25 MBq of [^{14}C]-radiolabeled afatinib (Boehringer Ingelheim Pharma GmbH & Co. KG, Biberach, Germany) in the sitting/standing position. The [^{14}C]-afatinib powder was reconstituted with 50 mL of isotonic sodium chloride solution. This solution was administered orally to the volunteers. The empty vial was rinsed once more with another 50 mL of isotonic sodium chloride solution, which was then administered to the subjects. Subjects remained in the study center for at least 120 h for the collection of blood, urine and feces samples. If the radioactivity counts measured in urine and feces from day 5 onwards remained above the termination limits (50 dpm/mL in urine and 75 dpm per 100 mg feces), the stay in the center was extended to a maximum of 10 days. Thereafter, collection of urine and/or feces was continued at home until the [^{14}C]-radioactivity quick counts fell below the termination criteria.

Sample collection

All blood samples were collected in potassium-EDTA-containing tubes. Venous blood samples for measurement of plasma levels of afatinib and [^{14}C]-radioactivity were obtained pre-dose and at 0.25, 0.5, 0.75, 1, 1.5, 2, 3, 4, 6, 8, 10, 12, 24, 36, 48, 72 and 96 h after dosing. For pharmacokinetic assessments, approximately 11 mL of blood was collected at each time point. A 2-mL aliquot was taken for

the determination of [^{14}C]-radioactivity in whole blood and stored at −20°C. The remaining 9 mL was centrifuged immediately at 2,000*g* (4°C) for 10 min. Two aliquots of at least 1 mL each were used for the determination of [^{14}C]-radioactivity in plasma, and 2 aliquots of at least 1 mL each were used for the analysis of the parent compound (afatinib) in plasma. Plasma aliquots were frozen immediately and stored at −20°C until analysis.

Additional blood samples were collected pre-dose and 1, 2 and 6 h after dosing for metabolic profiling (50 mL). Blood samples were centrifuged at 2,000*g* (4°C) for 10 min. Each blood cell pellet was divided into two approximately equal parts and transferred to two suitable storage tubes. The blood cell samples were stored at −20°C until shipment to the metabolic laboratory at Boehringer Ingelheim Pharma GmbH & Co. KG. Plasma was also transferred to separate tubes and stored at −20°C until shipment to the same laboratory.

Additional blood samples (10 mL) for the determination of protein binding were collected pre-dose and 1, 2 and 6 h after dosing. Blood samples were centrifuged at 2,000*g* (4°C) for 10 min. Plasma was transferred to separate tubes and stored at −20°C until shipment to the analytical laboratory at Pharma Bio-Research Group BV.

Hematocrit was determined in blood samples (2.5 mL) collected pre-dose and 1, 2 and 6 h after dosing.

Urine was collected in containers at pre-dose, 0–4, 4–8 and 8–24 h and then over 24-h intervals up to 120 h after dosing or until radioactivity in the sample was less than 50 dpm/mL. At the end of each collection period, the urine was homogenized and aliquots were taken for determination of [^{14}C]-radioactivity, afatinib concentrations and metabolic profiling. All samples were stored at −20°C. To ensure adequate excretion of [^{14}C]-afatinib, patients were advised to drink at least 2 liters of water per day.

Feces samples were collected throughout the study for the determination of total [^{14}C]-radioactivity concentrations and metabolic profiling. Samples were collected pre-dose and continuously over 24-h intervals up to 120 h after dosing or until radioactivity was less than 75 dpm per 100 mg sample. Samples were homogenized and prepared for the determination of [^{14}C]-radioactivity. All samples were stored at −20°C.

Analysis of afatinib concentration and radioactivity

Plasma and urine concentrations of afatinib were analyzed by validated high-performance liquid chromatography–tandem mass spectrometry (HPLC–MS/MS) after solid-phase extraction in the 96-well format. The internal standard was deuterated [D_6]afatinib. Chromatography was achieved on an analytical C18 reverse-phase HPLC column with gradient elution. The substance was detected and quantified by HPLC–MS/MS using electrospray ionization in the positive ion mode. The lower limit of quantification (LLQ) of afatinib was 0.1 ng/mL in plasma and 0.5 ng/mL in urine. Validation data documented adequate accuracy, precision and specificity of the HPLC–MS/MS assay employed for the study. Analysis was performed by Boehringer Ingelheim Pharma GmbH & Co. KG, Biberach, Germany.

Levels of radioactivity in plasma, whole blood, urine and feces were determined by validated liquid scintillation counting methods using [1-methyl-^{14}C]-caffeine as the internal standard and expressed as [^{14}C]-afatinib-equivalents (EQ). The LLQ for [^{14}C]-radioactivity was 25 dpm/mL for whole blood, 20 dpm/mL in plasma, 10 dpm/mL in urine and 40 dpm/mg in feces. This corresponds to a LLQ of 2.88 ngeq/mL for [^{14}C]-radioactivity in whole blood and 2.30 ngeq/mL for [^{14}C]-radioactivity in plasma (versus 0.1 ng/mL for afatinib in plasma). Validation data documented adequate accuracy, precision and specificity of the assay employed for the study.

Pharmacokinetic analysis

Standard non-compartmental methods were used to calculate pharmacokinetic parameters using WinNonlin® Professional Network version 5.0.1 (Pharsight Corporation, Cary, NC, USA). Area under the plasma concentration–time curve (AUC_{0-t_z}) was calculated using the log-linear trapezoidal rule up to the time of the last sampling point with a measurable plasma concentration. Terminal half-life was calculated from the terminal rate constant, and renal clearance ($CL_{R,0-96}$) was calculated as the amount of afatinib excreted in urine/plasma AUC over 96 h. Descriptive statistics were reported as the geometric mean and geometric coefficient of variation (CV).

Metabolite analysis

Metabolite patterns in plasma (pooled samples), urine and feces (samples from individual subjects) were analyzed by HPLC coupled to off-line (plasma) and on-line (urine, feces) radioactivity detection.

Urine and feces analysis

Urine samples were processed by solid-phase extraction on Discovery DSC-18LT (1 g, 6 mL) cartridges (Supelco, USA) preconditioned with 5 mL of methanol and equilibrated with 10 mL of 1% aqueous formic acid. After complete thawing, mixing and short centrifugation to remove any solids, samples (~100 mL) were acidified with 5 μL/mL of formic acid and applied to the extraction columns. After rinsing with 20 mL of water/methanol/

formic acid (90.9/9/0.1), the absorbed material was eluted with 10 mL of methanol/water/formic acid (94.9/5/0.1) and the eluate was concentrated under a stream of nitrogen to near dryness. The average extraction yield was 97% (range 82% to 105%).

Feces homogenates were processed by liquid extraction. After complete thawing and mixing of the feces homogenates, 2 g of samples was extracted (15 min vigorous shaking, followed by centrifugation for 5 min at 400×*g*) 3 times with 3 mL of methanol/acetonitrile/water/formic acid (48/48/3.9/0.1) and once with 3 mL of methanol/acetonitrile/water/ammonium hydroxide (48/48/3.9/0.1). The extracts were combined and concentrated under a stream of nitrogen to about 1 mL. The liquid residues were transferred into plastic vials, and solid residues were extracted with 2 mL of methanol/acetonitrile/water (45/50/5); after a short centrifugation, the supernatants were also transferred into vials. The combined samples were reduced with nitrogen to about 1 mL. The average extraction yield was 78% (range 69% to 86%).

Sample aliquots (urine or feces) of 100 µL were quantitatively injected into the HPLC with on-line detection operated by Chromeleon, version 3.05 (Dionex, Idstein, Germany). Samples were analyzed on 150 × 4.6 mm ProC18 HD columns protected by 10 × 4 mm ProC18 RS guard columns (both 5 µm particle size; YMC, Germany). Metabolites were separated with a gradient of aqueous ammonium acetate (0.1 M, pH 8.5 adjusted with ammonium hydroxide: mobile phase A) versus acetonitrile (mobile phase B) at a flow rate of 1.0 mL/min (gradient: 5% B at 0 min, linear to 25% B at 5 min, linear to 31% B at 25 min, linear to 55% B at 38 min, linear to 95% B at 39 min with plateau at 95% B to 42 min). With a signal-to-noise ratio $S/N = 2$, the detection system was linear ($r^2 \geq 0.99$) over the range of 329–374183 dpm (absolute amount injected on column), respectively, as assessed by triplicate injections of [^{14}C]-afatinib at various concentrations. The radioactivity of aliquots of urine or feces samples, rinsing solutions, eluates and reconstituted solutions for HPLC analysis was determined by liquid scintillation counting.

Plasma analysis

Plasma samples obtained at 1, 2 and 6 h after oral administration of [^{14}C]-afatinib were processed by solid-phase extraction on Discovery DSC-18LT (2 g, 12 mL) cartridges (Supelco, USA) preconditioned with 5 mL of acetonitrile and equilibrated with 10 mL of water. Samples (~40 mL) were acidified with 0.1 M hydrochloric acid (4 + 1) and, after mixing and short centrifugation to remove any solids, were applied onto the columns. After rinsing with 10 mL methanol/acetonitrile/water (90/10 v/v) and drying, the absorbed material was eluted twice with 10 mL of methanol/acetonitrile/water (48.5/48.5/3), and the combined eluates were concentrated under a stream of nitrogen to near dryness. The liquid residues were transferred into plastic vials, and the solid residues were extracted twice with 1 mL of methanol/water (90/10); then, after short centrifugation, the supernatants were also transferred into vials. These combined samples were reduced to about 200 µL. The average extraction yield was 103% (range 94% to 108%).

Sample aliquots of 100 µL were injected into the HPLC off-line detection system (low level counting). The HPLC system used the same gradient as for the on-line radioactivity detection analyses and MassLynx and FractionLynx software (version 4, Waters, Germany). The post-column flow was sampled in 7-sec intervals into 96-well plates (Deepwell LumaPlates, Perkin Elmer, Belgium), which were preconditioned with a solid-phase scintillator. After evaporation of the solvent to dryness, the plates were analyzed by scintillation counting in an LSC microplate counter (TopCount NXT, Perkin Elmer, USA). The LLQ for plasma samples was 38 dpm, which was equivalent to a concentration of a defined radioactive component of approximately 0.06 ngeq/mL when 100 mL of plasma was extracted for a single HPLC run. Metabolites were quantified on the basis of the relative amount of radioactivity that was assigned to a given metabolite fraction in relation to the total amount of radioactivity present in the analyzed sample. Parent drug and metabolites were expressed as percentage of sample radioactivity in plasma or as percentage of the dose in excreta. The radioactivity of aliquots of plasma samples, rinsing solutions, eluates and reconstituted solutions for HPLC analysis was determined by liquid scintillation counting.

Determination of covalent binding in blood cells and plasma

Hemolyzed blood samples and pooled plasma were separately precipitated and extracted using threefold volume of ice-cold acetonitrile with 5% glacial acetic acid. After centrifugation (5 min at 4,000×*g*), the supernatants were removed and the residual pellet was re-suspended in acetonitrile/5% glacial acetic acid. This extraction step was repeated twice for the separate samples, and then the supernatants were combined. The residual plasma protein pellet was dissolved in 1 M sodium hydroxide solution, and residual blood pellets were transferred into combustion cones. For plasma samples, the amount of extractable radioactivity in the supernatants and the amount of covalent bound radioactivity in the residual pellets were determined by liquid scintillation counting. For blood cells, radioactivity of aliquots of the hemolyzed blood cells, the supernatants and the residual pellets was determined by combustion analysis and liquid scintillation counting.

Metabolite identification

Aliquots of plasma, urine, and feces samples were analyzed by electrospray ionization mass spectrometry in the positive ion mode using a quadrupole orthogonal acceleration time-of-flight mass spectrometer (Micromass, Manchester, UK). Argon was used as collision gas. The time-of-flight analyzer operated at a mass resolution $m/\Delta m = 10{,}000$ in V-ion optics mode with a pusher frequency of 16 kHz. The scan time in MS mode and MS/MS mode was 1 s/scan. Exact mass measurements in MS and MS/MS operations were taken by internal calibration with phosphoric acid (0.01%) in positive ion mode using an electrospray ionization/lockspray interface.

Metabolite structures were elucidated by LC–MS of the radioactive metabolite peaks, with exact mass measurements and detailed analysis of the fragmentation process of pseudomolecular metabolite ions $[M+H]^+$ and their product ions generated by collision induced fragmentation. The exact mass measurements were performed on a quadrupole orthogonal acceleration time-of-flight instrument with V- and W-optics coupled with an ESI interface using a reverse-phase HPLC system.

MS/MS experiments for structure elucidation were performed on representative samples. When available, the identity of metabolites was confirmed by exact mass measurements of the pseudomolecular [M+H]+-metabolite ions and by comparison of MS/MS data and retention times of synthetic reference compounds. The assignment of metabolite structures was confirmed by comparison of LC–MS data of previous metabolism studies in rats and minipigs after administration of ^{14}C-labeled afatinib (Boehringer Ingelheim, data on file) and in humans following administration of non-labeled afatinib [5].

Results

Pharmacokinetics

Afatinib was slowly absorbed with maximum plasma concentration of afatinib and [^{14}C]-radioactivity in plasma and whole blood achieved at a median of 6 h after dosing (Table 1). Due to differences in the LLQ ranges of the bioanalytical assays for afatinib in plasma, for [^{14}C]-radioactivity in plasma and for [^{14}C]-radioactivity in whole blood, there were differences in the absorption phases of afatinib compared to [^{14}C]-radioactivity in plasma and whole blood. The shapes of the afatinib plasma, [^{14}C]-plasma and [^{14}C]-whole blood radioactivity concentration–time profiles were similar up to 12 h post-dose (Fig. 1). After 12 h, the afatinib plasma concentrations declined more rapidly than the [^{14}C]-plasma radioactivity and [^{14}C]-whole-blood radioactivity profiles. Total [^{14}C]-radioactivity concentrations in plasma were higher than afatinib plasma concentrations, indicating the presence of one or more metabolites other than afatinib (*refer to metabolite profiling results below*). The geometric mean blood to plasma [^{14}C]-radioactivity concentration ratio at 6 h post-dose was 1.28 (range 0.935 to 1.94, geometric CV 25.1%).

Afatinib accounted for 72.9% of total [^{14}C]-radioactivity in plasma in the first 24 h after dosing (Table 1). Around 80% of the AUC_{0-24} of [^{14}C]-radioactivity in whole blood was found in plasma. The proportion of afatinib exposure

Table 1 Comparison of pharmacokinetic parameters of afatinib in plasma and radiolabeled [^{14}C]-afatinib-equivalent (EQ) in plasma and whole blood after single oral administration of 15 mg afatinib (2.25 MBq [^{14}C]-labeled afatinib) solution in 8 healthy male volunteers

Parameters	Afatinib in plasma		[^{14}C]-afatinib-EQ in plasma		[^{14}C]-afatinib-EQ in whole blood	
	Units	gMean (gCV [%])	Units	gMean (gCV [%])	Units	gMean (gCV [%])
AUC_{0-24}	[ng h/mL]	80.2 (34.9)	[ngeq h/mL]	110 (40.1)	[ngeq h/mL]	138 (47.1)
AUC_{0-tz}[a]	[ng h/mL]	144 (32.3)	[ngeq h/mL]	231 (69.9)	[ngeq h/mL]	446 (59.1)
C_{max}	[ng/mL]	6.19 (38.4)	[ngeq/mL]	7.58 (36.0)	[ngeq/mL]	8.01 (41.2)
t_{max}[b]	[h]	6.00 (1.50–8.02)	[h]	6.00 (0.750–8.02)	[h]	6.00 (0.750–6.08)
$t_{½}$	[h]	33.9 (14.3)	[h]	118 (65.1)	[h]	195 (83.9)
CL/*F*	[mL/min]	1,530 (31.2)	[mL/min]	325 (51.1)	[mL/min]	141 (104)
V_z/F	[L]	4,500 (37.6)	[L]	3,330 (37.1)	[L]	2,390 (34.8)

AUC_{0-24} area under the concentration–time curve from zero time to 24 h, AUC_{0-t_z} area under the plasma concentration–time curve from zero time to time of the last quantifiable drug plasma concentration, C_{max} maximum observed concentration, t_{max} time at which observed C_{max} occurred, $t_{½}$ terminal half-life, CL/F total body clearance, V_z/F apparent volume of distribution during the terminal phase, gCV geometric coefficient of variation

[a] $t_z = 96$ h for $N = 8$ for afatinib in plasma; $t_z = 96$ h for $N = 2$, 72 h for $N = 3$, 48 h for $N = 2$ and 24 h for $N = 1$ for [^{14}C]-afatinib-EQ in plasma; $t_z = 96$ h for $N = 6$, 72 h for $N = 1$, and 48 h for $N = 1$ for [^{14}C]-afatinib-EQ in whole blood

[b] Median and range

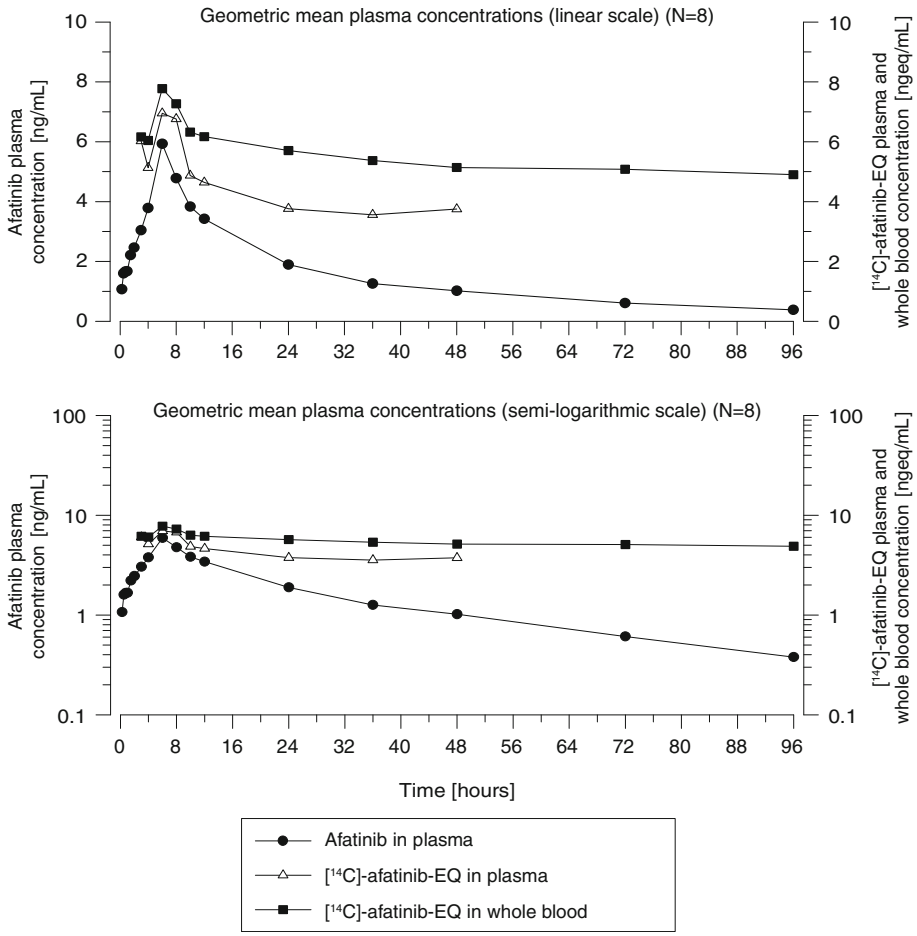

Fig. 1 Geometric mean concentration–time profiles of afatinib in plasma, radiolabeled [^{14}C]-afatinib-equivalent (EQ) in plasma and [^{14}C]-afatinib-EQ in whole blood after single oral administration of 15 mg afatinib (2.25 MBq [^{14}C]-labeled afatinib) solution in 8 healthy volunteer subjects (*top graph* linear scale; *bottom graph* semilogarithmic scale, both with time axis limited to 96 h)

in plasma until the last measurable concentration (AUC_{0-t_z}) was lower compared with the respective radioactivity exposure in plasma seen within the first 24 h (AUC_{0-24} [^{14}C]-afatinib-EQ). Thus, at later time points (>24 h after dosing), the proportion of [^{14}C]-radioactivity in plasma increased relative to afatinib concentrations in plasma, in contrast to that observed in the first 24 h.

The contribution of renal excretion to total body clearance of [^{14}C]-radioactivity was low (Fig. 2). The fraction excreted via the urine as unchanged afatinib by 120 h postdose was 0.687% compared with 3.11% total [^{14}C]-radioactivity in urine at the same time point (Table 2). By 216 h after dosing (last point of measurement), total [^{14}C]-radioactivity excreted in the urine was 4.29%. Renal clearance over the time interval of 0–96 h ($CL_{R,0-96}$) was lower for afatinib (11.4 mL/min) compared with [^{14}C]-radioactivity in plasma (22.4 mL/min). As shown in Figs. 3 and 4, the major route of excretion of total [^{14}C]-radioactivity was via feces, with 85.4% excreted within 312 h after dosing. Overall mean recovery of [^{14}C]-radioactivity up to 312 h after dosing was 89.5% (Fig. 4).

The mean terminal half-life was 33.9 h for afatinib, 118 h for [^{14}C]-radioactivity in plasma and 195 h for [^{14}C]-radioactivity in whole blood (Table 1). Apparent total body clearance (CL/F) for afatinib in plasma was high (mean 1,530 mL/min) compared with that for [^{14}C]-radioactivity in plasma and whole blood (325 and 141 mL/min, respectively). Afatinib also exhibited a high apparent oral volume of distribution (V_z/F) during the terminal phase (4,500 L). By comparison, mean apparent V_z/F for [^{14}C]-radioactivity in plasma (3,330 L) was higher than the one for [^{14}C]-radioactivity in whole blood (2,390 L) (Table 1).

The results of the plasma protein binding of [^{14}C]-radioactivity were all in the lower part of the validated range and were therefore not regarded as informative.

Metabolite profiles in plasma, urine and feces

The parent compound afatinib was the most prevalent compound, comprising approximately 89% of excreted radioactivity. Metabolism as an elimination pathway in excreta (in either urine or feces) was of subordinate importance compared with the excretion of the unchanged parent compound (data not shown). Of the metabolites accounting for >1% of the dose, only various adducts of afatinib to glutathione, cysteine–glycine or cysteine were

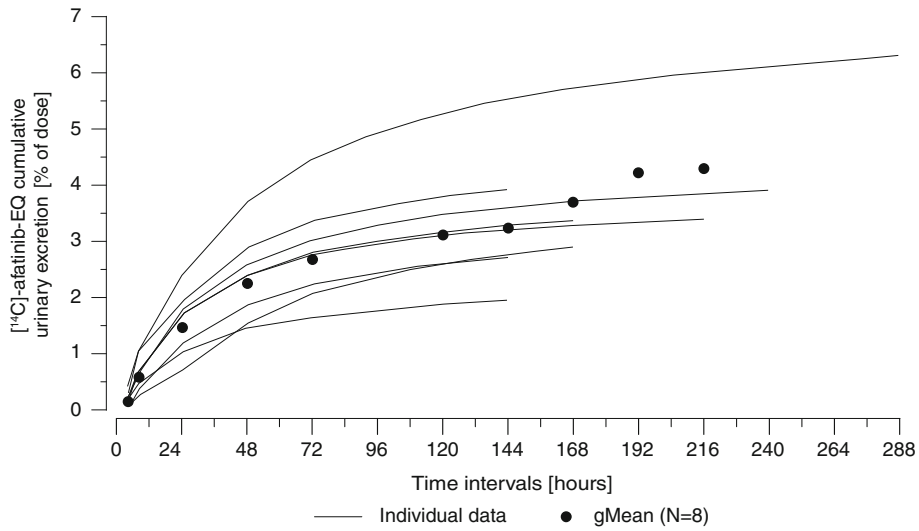

Fig. 2 Individual and geometric mean cumulative urinary excretion of radiolabeled [^{14}C]-afatinib-equivalent (EQ) as percent of dose after single oral administration of 15 mg afatinib (2.25 MBq [^{14}C]-labeled afatinib) solution in 8 healthy volunteer subjects

Table 2 Comparison of pharmacokinetic parameters of afatinib in urine and radiolabeled [^{14}C]-afatinib-equivalent (EQ) in urine and feces after single oral administration of 15 mg afatinib (2.25 MBq [^{14}C]-labeled afatinib) solution in 8 healthy volunteer subjects

Parameters	Afatinib in urine		[^{14}C]-afatinib-EQ in urine		[^{14}C]-afatinib-EQ in feces ($N = 7$)[a]	
	Units	gMean (gCV [%])	Units	gMean (gCV [%])	Units	gMean (gCV [%])
$Ae_{0–120}$	[μg]	103 (54.9)	[μgeq]	467 (31.9)	[μgeq]	–
$fe_{0–120}$	[%]	0.687 (55.0)	[%]	3.11 (31.3)	[%]	–
$CL_{R,0–96}$	[mL/min]	11.4 (45.2)	[mL/min]	22.4 (19.2)	[mL/min]	–
$Ae_{0–312,\ feces}$	[μgeq]	–	[μgeq]	–	[μgeq]	12,800 (5.79)
$fe_{0–312,\ feces}$	[%]	–	[%]	–	[%]	85.4 (5.82)

$Ae_{0–120}$ amount of afatinib or its metabolites excreted in urine during the interval of 0–120 h, $fe_{0–120}$ fraction of analyte eliminated in urine during the interval of 0–120 h, $CL_{R,0–96}$ renal clearance during the interval of 0–96 h, $Ae_{0–312,\ feces}$ amount of analyte eliminated in feces during the interval of 0–312 h, $fe_{0–312,\ feces}$ fraction of analyte eliminated in feces during the interval of 0–312 h, gCV geometric coefficient of variation

[a] Urine from subjects 4 and 5 was combined for the time interval 72–96 h

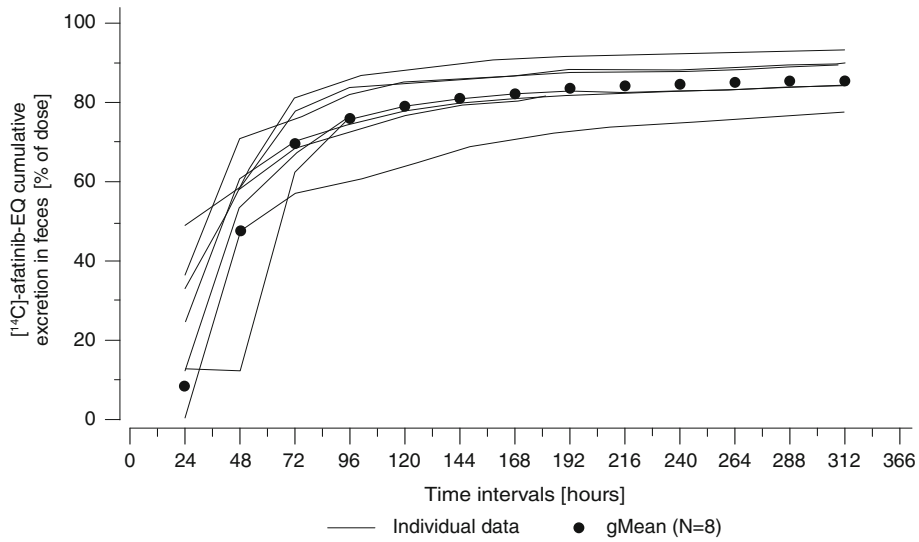

Fig. 3 Individual and geometric mean cumulative excretion of radiolabeled [^{14}C]-afatinib-equivalent (EQ) as percent of dose in feces after single oral administration of 15 mg afatinib (2.25 MBq [^{14}C]-labeled afatinib) solution in 8 healthy volunteer subjects

detected in the urine and feces. Except for minor amounts of the dimethylamino N-oxide, all metabolites were conjugates formed by Michael addition. A general scheme for the formation of such conjugated metabolites of afatinib to nucleophilic components by Michael addition is depicted in Fig. 5.

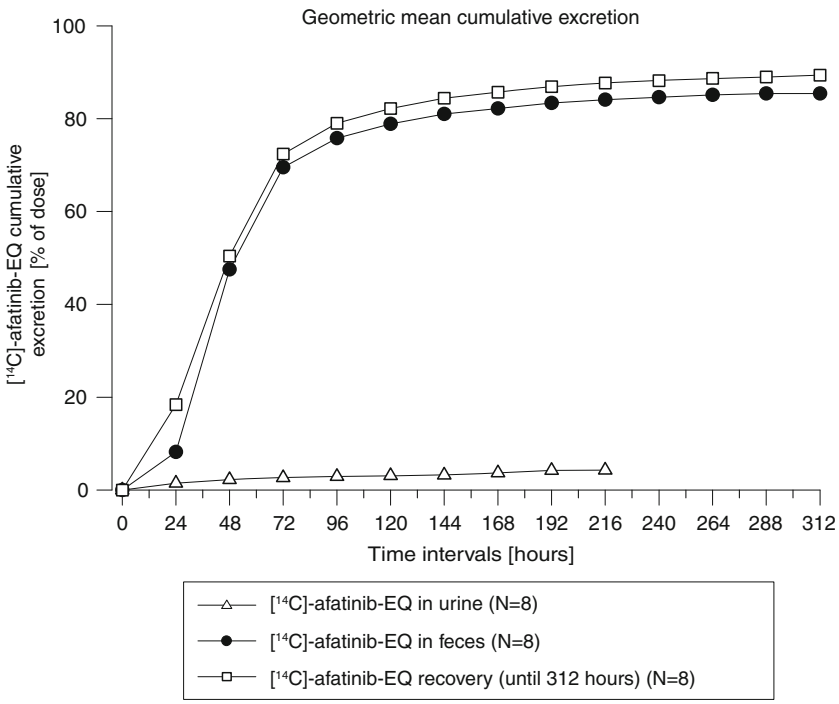

Fig. 4 Geometric mean cumulative excretion of radiolabeled [^{14}C]-afatinib-equivalent (EQ) as percent of dose in urine, feces and recovery up to 312 h after single oral administration of 15 mg afatinib (2.25 MBq [^{14}C]-labeled afatinib) solution in 8 healthy volunteer subjects

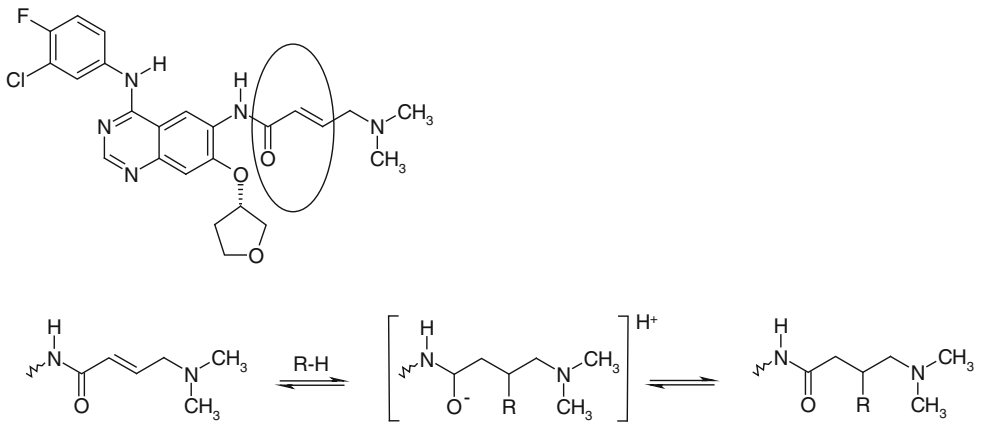

Fig. 5 Principal metabolic pathway of afatinib in humans. The encircled α,β-unsaturated ketone moiety undergoes Michael addition with suitable electron-rich reactants, such as glutathione, cysteine yielding conjugate metabolites or functional groups of proteins resulting in the formation of protein adducts. The general scheme of a Michael addition is displayed in which R–H represents the electron-rich reactants, yielding conjugate metabolites. If R–H is part of an electron-rich (e.g., sulfhydryl or amino group) functional moiety of proteins, Michael addition will yield covalent protein adducts of afatinib

Plasma samples collected 1, 2 and 6 h after oral dosing contained very low concentrations of radioactivity (2.79-10.2 ngeq/mL). This precluded the investigation of individual samples, and therefore, samples were pooled according to the sampling time for the assessment of metabolite patterns. [^{14}C]-afatinib was the predominant radioactive compound in the pooled plasma samples, accounting for >97% of the total sample radioactivity. No circulating metabolites of afatinib were identified by high-resolution LC–MS (detection limit ~0.06 ngeq/mL). A substantial part of the radioactivity in the plasma samples was found to be covalently bound to plasma proteins. This fraction increased with sampling time, from 7% at 1–2 h to 48% of total sample radioactivity at 72 h (Fig. 6). Substantial amounts of covalently bound radioactivity were also observed in samples of hemolyzed blood cells. Depending on the sampling time, 65–77% of the total radioactivity in the samples was bound to blood cell proteins. However, absolute concentrations of these adducts were small and did not exceed 1.6 ngeq/mL for plasma samples.

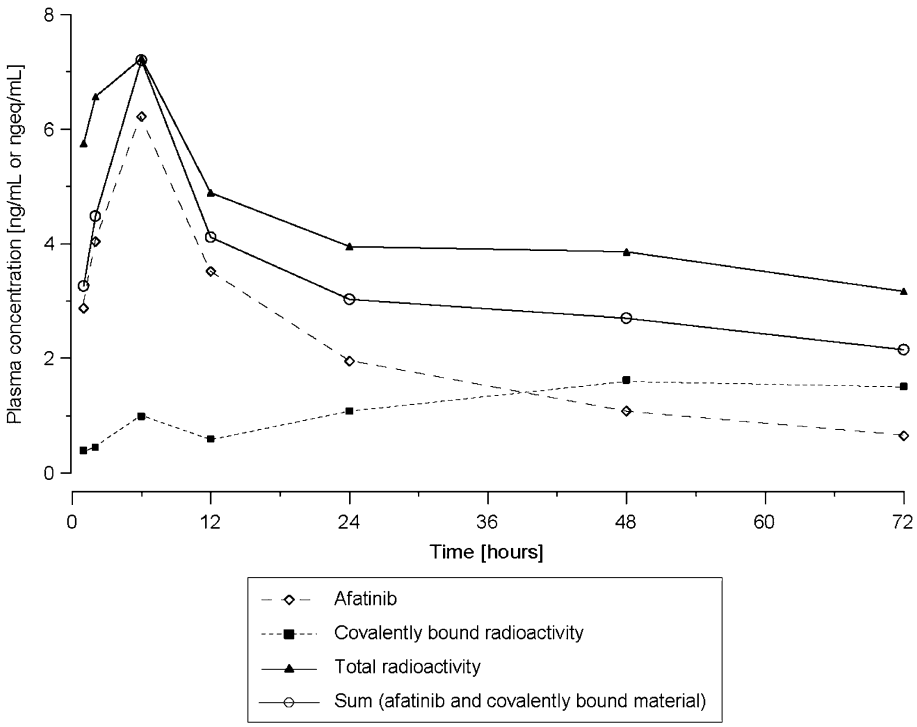

Fig. 6 Plasma concentration versus time profile for afatinib, covalently bound radioactivity and total radioactivity from healthy male subjects after a single 15 mg dose of [^{14}C]-afatinib

Tolerability

Seven subjects experienced at least one adverse event after dosing. Possible drug-related events included abdominal distension (2 subjects, one also experienced abdominal discomfort) and one subject each with fatigue, somnolence or frequent bowel movements. All adverse events were of CTCAE (**common terminology criteria for adverse events)** grade 1. All subjects recovered completely without the need for therapeutic intervention.

Discussion

This study investigated the pharmacokinetic characteristics, the routes of elimination and metabolic profile of [^{14}C]-afatinib in healthy male volunteers. After oral administration of afatinib, most of the recovered dose was in feces (85.4%), with urinary excretion representing a minor elimination pathway (4.29%). The overall recovery of 89.5% of the radioactive dose indicates a complete mass balance with most of the recovery occurring within 72 h of dosing.

Values obtained for time to reach maximum plasma concentrations, maximum plasma concentration, area under the plasma concentration time curve and terminal half-life in this healthy volunteer study were comparable with those observed in cancer patients [5]. The ratio of AUC_{0-t_z} for [^{14}C]-radioactivity in whole blood to plasma suggests that a considerable part of the [^{14}C]-radioactivity is related to afatinib metabolite(s) in whole blood or to afatinib itself bound to whole-blood components. However, caution is required in the interpretation of these results since the AUC_{0-t_z} for [^{14}C]-afatinib-EQ in plasma and whole blood could not be calculated for all patients at 96 h (see Table 1 legend), since the [^{14}C]-afatinib-EQ concentrations in plasma and whole blood were already near the LLQ after 24 h. Values for total afatinib exposure ($AUC_{0-\infty}$) and total [^{14}C]-radioactivity exposure in plasma and whole blood were not reported, since the $\%AUC_{t_z-\infty}$ for [^{14}C]-radioactivity in plasma and whole blood were 64.0% and 70.6%, respectively, and were therefore regarded as uncertain. The mean terminal half-life for [^{14}C]-radioactivity in plasma and whole blood was longer than that observed for afatinib in plasma (Table 1), suggestive of the presence of one or more metabolite(s) of afatinib in plasma and in whole blood with a longer terminal half-life than afatinib. Higher total [^{14}C]-radioactivity concentration in whole blood than plasma was indicative of distribution of afatinib and/or its metabolites into red blood cells. The terminal half-life of [^{14}C]-radioactivity in plasma and in whole blood may have been underestimated due to the limited sampling time within this trial (up to 96 h), and evidence that [^{14}C]-radioactivity in plasma and whole blood was already near the LLQ by 24 h after dosing. Very high values for apparent total body clearance and volume of distribution for afatinib in plasma during the terminal phase were suggestive of high tissue distribution of the drug. Comparison of the mean apparent V_z/F for [^{14}C]-radioactivity in plasma and for [^{14}C]-radioactivity in whole blood indicated that

metabolite(s) of afatinib in plasma and in whole blood have a lower volume of distribution than afatinib itself (Table 1). However, these absolute values should be treated with caution as the absolute bioavailability of afatinib in humans is unknown. Moderate distribution of [^{14}C]-radioactivity into red blood cells was noted.

Similar to the results seen in this trial, oral administration of [^{14}C]-radiolabeled gefitinib or [^{14}C]-radiolabeled erlotinib, other EGFR inhibitors with comparable structures to afatinib, show predominant excretion of [^{14}C]-radioactivity in humans via the feces with only minor amounts excreted in the urine [17, 18].

Metabolite profiling studies show that the parent compound (afatinib) is the major drug-related component in plasma, urine and feces in humans. Metabolism of afatinib was minimal with covalent binding to plasma proteins representing the predominant fraction in plasma after 36 h. Almost the entire circulating radioactivity in the plasma was accounted for by the parent drug (afatinib) or covalent adducts. In urine and feces, the parent compound accounted for 89% of the excreted drug-related material.

There was some discrepancy in the data for total [^{14}C]-radioactivity in plasma based on the analytical methods used (Figs. 1, 6). [^{14}C]-radioactivity concentrations were very low, causing technical difficulties in the quantitative assessment of [^{14}C]-radioactivity in plasma (and whole blood) and one of the possible metabolites. Consequently, variability for [^{14}C]-radioactivity in plasma (and whole blood) was higher than that observed using more conventional bioanalytical methods. Additionally, the available sample volumes were insufficient to allow for analysis of samples from individual donors or, indeed, for multiple re-analyses of the pooled plasma samples. Therefore, we cannot exclude the possibility that the somewhat higher [^{14}C]-radioactivity in plasma (Fig. 1 vs. Fig. 6) may have been due to variability in the analytical method and extensive sample work-up.

The proposed scheme of conjugative metabolism of afatinib (Fig. 5), shows that the structure of afatinib comprises an α, β-unsaturated ketone moiety that can act as the acceptor molecule of a Michael addition. This property of afatinib resulted in the formation of covalent adducts to protein and nucleophilic, electron-rich small molecules (such as SH-containing small molecules, e.g., cysteine, glutathione) (Boehringer Ingelheim, data on file). For plasma proteins, this was shown in vivo in animals and humans (Boehringer Ingelheim, data on file). Therefore, covalent binding to plasma proteins and erythrocytes may serve as an explanation for the long terminal half-life of radioactivity in plasma and blood observed during this study. Although the potential exists for allergic reactions if the drug acts like a hapten, this has not been observed in patients receiving afatinib. Covalent binding to human serum albumin has also been reported for another HER-2 tyrosine kinase inhibitor HKI-272 with a structure closely related to afatinib [19].

The absence of detectable CYP-mediated metabolism suggests that the risk of potential interaction between afatinib and other therapies metabolized by CYP450 enzymes (i.e., CYP substrates, CYP inhibitors and CYP inducers) is minimal. This finding is likely to be a clinical advantage, since agents interacting via the CYP450 enzyme system are widely used in the treatment for lung cancer patients [20]. In contrast, other tyrosine kinase inhibitors (notably erlotinib, gefitinib and lapatinib) are all metabolized by CYP3A4.

In conclusion, this study showed that afatinib was mainly eliminated unchanged via feces. Overall recovery of [^{14}C]-radioactivity was 89.5%, indicating a complete mass balance. Renal excretion was low, and no major circulating metabolites were identified. Metabolism therefore plays a negligible role in the overall disposition and elimination of afatinib in humans. Oral single-dose administration of afatinib was well tolerated.

Acknowledgments This study was supported by Boehringer Ingelheim. Editorial assistance was provided with funding from Boehringer Ingelheim.

Conflict of interest All authors are employees of Boehringer Ingelheim.

References

1. Li D, Ambrogio L, Shimamura T, Kubo S, Takahashi M, Chirieac LR, Padera RF, Shapiro GI, Baum A, Himmelsbach F, Rettig WJ, Meyerson M, Solca F, Greulich H, Wong KK (2008) BIBW2992, an irreversible EGFR/HER2 inhibitor highly effective in preclinical lung cancer models. Oncogene 27(34):4702–4711
2. Bahleda R, Soria J, Berge Y, Massard C, Wind S, Uttenreuther-Fischer MM, Fleischer F, De-Montserrat H, Solca F, Tschoepe I, Delord J (2011) Phase I trial assessing safety and pharmacokinetics of afatinib (BIBW 2992) with intravenous weekly vinorelbine in advanced solid tumors (abstract). J Clin Oncol 29(15 Suppl):2585
3. Agus DB, Terlizzi E, Stopfer P, Amelsberg A, Gordon MS (2006) A phase I dose escalation study of BIBW 2992, an irreversible dual EGFR/HER2 receptor tyrosine kinase inhibitor, in a continuous schedule in patients with advanced solid tumours (abstract 2074). J Clin Oncol 24(18 Suppl):97S
4. Lewis N, Marshall J, Amelsberg A, Cohen RB, Stopfer P, Hwang J, Malik S (2006) A phase I dose escalation study of BIBW 2992, an irreversible dual EGFR/HER2 receptor tyrosine kinase inhibitor, in a 3 week on 1 week off schedule in patients with advanced solid tumors (abstract 3091). J Clin Oncol 24(18 Suppl):143S
5. Eskens FA, Mom CH, Planting AS, Gietema JA, Amelsberg A, Huisman H, van Doorn L, Burger H, Stopfer P, Verweij J, de Vries EG (2008) A phase I dose escalation study of BIBW 2992, an irreversible dual inhibitor of epidermal growth factor receptor 1 (EGFR) and 2 (HER2) tyrosine kinase in a 2-week on, 2-week off schedule in patients with advanced solid tumours. Br J Cancer 98(1):80–85

6. Yap TA, Vidal L, Adam J, Stephens P, Spicer J, Shaw H, Ang J, Temple G, Bell S, Shahidi M, Uttenreuther-Fischer M, Stopfer P, Futreal A, Calvert H, de Bono JS, Plummer R (2010) Phase I trial of the irreversible EGFR and HER2 kinase inhibitor BIBW 2992 in patients with advanced solid tumors. J Clin Oncol 28(25): 3965–3972
7. Ang J, Mikropoulos C, Stavridi F, Rudman S, Uttenreuther-Fisher M, Shahidi M, Pemberton K, Wind S, de Bono J, Spicer JF (2009) A phase I study of daily BIBW 2992, an irreversible EGFR/HER-2 dual kinase inhibitor, in combination with weekly paclitaxel (abstract). J Clin Oncol 27(15):e14541
8. Awada AH, Dumez H, Wolter P, Hendlisz A, Besse-Hammer T, Piccart M, Uttenreuther-Fischer M, Stopfer P, Taton M, Schoffski P (2009) A phase I dose finding study of the 3-day administration of BIBW 2992, an irreversible dual EGFR/HER-2 inhibitor, in combination with three-weekly docetaxel in patients with advanced solid tumors (abstract). J Clin Oncol 27(15 Suppl):3556
9. Vermorken JB, Machiels JH, Rottey S, Thurm HC, Pelling K, Lahogue A (2010) Phase Ib study evaluating the combination of BIBW 2992 with two different standard chemotherapy regimens, cisplatin/paclitaxel (PT) and cisplatin/5-FU (PF), in patients with advanced solid tumors (abstract). J Clin Oncol 28(15 Suppl):e13521
10. Miller VA, Hirsh V, Cadranel J, Chen Y-M, Park K, Kim S-W, Caicun Z, Oberdick M, Shahidi M, Yang C-H (2010) Phase IIB/III double-blind randomized trial of afatinib (BIBW 2992, an irreversible inhibitor of EGFR/HER1 and HER2) + best supportive care (BSC) versus placebo 1 + BSC in patients with NSCLC failing 1-2 lines of chemotherapy and erlotinib or gefitinib (LUX-LUNG 1) [abstract LBA1]. Ann Oncol 21(Suppl 8):viii1
11. Yang CH, Shih JY, Su WC, Hsia TC, Sequist LV, Chang GC, Calvo R, Cong XJ, Shahidi M, Miller VA (2010) A Phase II study of afatinib (BIBW 2992) in patients with adenocarcinoma of the lung and activating EGFR/HER1 mutations (LUX-Lung 2) [abstract O-042]. J Thorac Oncol 5(12):S376–S377
12. Hickish T, Wheatley D, Lin N, Carey L, Houston S, Mendelson D, Solca F, Uttenreuther-Fischer M, Jones H, Winer E (2009) Use of BIBW 2992, a novel irreversible EGFR/HER1, HER2 tyrosine kinase inhibitor to treat patients with HER2-Positive metastatic breast cancer after failure of treatment with trastuzumab (abstract 5060). Cancer Res 69(24):785S
13. Ranson M, Hammond LA, Ferry D, Kris M, Tullo A, Murray PI, Miller V, Averbuch S, Ochs J, Morris C, Feyereislova A, Swaisland H, Rowinsky EK (2002) ZD1839, a selective oral epidermal growth factor receptor-tyrosine kinase inhibitor, is well tolerated and active in patients with solid, malignant tumors: results of a phase I trial. J Clin Oncol 20(9):2240–2250
14. Baselga J, Rischin D, Ranson M, Calvert H, Raymond E, Kieback DG, Kaye SB, Gianni L, Harris A, Bjork T, Averbuch SD, Feyereislova A, Swaisland H, Rojo F, Albanell J (2002) Phase I safety, pharmacokinetic, and pharmacodynamic trial of ZD1839, a selective oral epidermal growth factor receptor tyrosine kinase inhibitor, in patients with five selected solid tumor types. J Clin Oncol 20(21):4292–4302
15. Hidalgo M, Bloedow D (2003) Pharmacokinetics and pharmacodynamics: maximizing the clinical potential of Erlotinib (Tarceva). Semin Oncol 30(3 Suppl 7):25–33
16. Burris HA 3rd, Hurwitz HI, Dees EC, Dowlati A, Blackwell KL, O'Neil B, Marcom PK, Ellis MJ, Overmoyer B, Jones SF, Harris JL, Smith DA, Koch KM, Stead A, Mangum S, Spector NL (2005) Phase I safety, pharmacokinetics, and clinical activity study of lapatinib (GW572016), a reversible dual inhibitor of epidermal growth factor receptor tyrosine kinases, in heavily pretreated patients with metastatic carcinomas. J Clin Oncol 23(23):5305–5313
17. McKillop D, Hutchison M, Partridge EA, Bushby N, Cooper CM, Clarkson-Jones JA, Herron W, Swaisland HC (2004) Metabolic disposition of gefitinib, an epidermal growth factor receptor tyrosine kinase inhibitor, in rat, dog and man. Xenobiotica 34(10):917–934
18. Ling J, Johnson KA, Miao Z, Rakhit A, Pantze MP, Hamilton M, Lum BL, Prakash C (2006) Metabolism and excretion of erlotinib, a small molecule inhibitor of epidermal growth factor receptor tyrosine kinase, in healthy male volunteers. Drug Metab Dispos 34(3):420–426
19. Wang J, Li-Chan XX, Atherton J, Deng L, Espina R, Yu L, Horwatt P, Ross S, Lockhead S, Ahmad S, Chandrasekaran A, Oganesian A, Scatina J, Mutlib A, Talaat R (2010) Characterization of HKI-272 covalent binding to human serum albumin. Drug Metab Dispos 38(7):1083–1093
20. Song X, Varker H, Eichelbaum M, Stopfer P, Shahidi M, Wilson K, Kaiser R, Finnern HW (2011) Treatment of lung cancer patients and concomitant use of drugs interacting with cytochrome P450 isoenzymes. Lung Cancer 74(1):103–111